Vibrio campbellii DS40M4 is a tractable model strain that diverges from the canonical quorum-sensing regulatory circuit in vibrios

Chelsea A. Simpson[†1], Blake D. Petersen[†1], Logan J. Geyman[1], Aimee H. Lee[1], Michael P. Manzella[1], Kai Papenfort[2,3], Julia C. van Kessel*[1]

1. Department of Biology, Indiana University, Bloomington, IN 47405
2. Friedrich Schiller University, Institute of Microbiology, 07745 Jena, Germany
3. Microverse Cluster, Friedrich Schiller University Jena, 07743 Jena, Germany.

[†]These authors contributed equally to this work.

* Corresponding author:
Email: jcvk@indiana.edu
Telephone: 812-856-2235
Fax: 812-856-5710

Running title: *V. campbellii* DS40M4 as a model bacterium

Keywords: quorum sensing, *Vibrio*, *Vibrio campbellii*, natural transformation, biofilm, type VI secretion, protease

Abstract

Vibrio campbellii BB120 (previously designated as *Vibrio harveyi*) is a fundamental model strain for studying population density-based cell-to-cell communication, known as quorum sensing. In *V. campbellii* BB120, sensing of autoinducers at high cell densities activates the expression of the master transcriptional regulator, LuxR, which controls the expression of genes involved in group behaviors. The environmental isolate *Vibrio campbellii* DS40M4 was recently shown to be capable of natural transformation, a process by which bacteria take up exogenous DNA and incorporate it into their genome via homologous recombination. In contrast, BB120 is not naturally transformable. Here, we compare additional phenotypes between these two *V. campbellii* strains. DS40M4 has a faster growth rate and stronger type VI secretion-mediated cell killing, whereas BB120 forms more robust biofilms and is bioluminescent. To explore the function of DS40M4-encoded homologs of the BB120 quorum-sensing system, we exploited the power of natural transformation to rapidly generate >30 mutant strains. Our results show that DS40M4 has a similar quorum-sensing circuit to BB120 but with three distinct differences: 1) DS40M4 lacks the canonical HAI-1 autoinducer LuxM synthase but has an active LuxN receptor, 2) the quorum regulatory small RNAs (Qrrs) are not solely regulated by autoinducer signaling through the response regulator LuxO, and 3) the DS40M4 LuxR regulon is <100 genes, which is relatively small compared to the >400 genes regulated in BB120. This work illustrates that DS40M4 is a tractable and relevant model strain for studying quorum-sensing phenotypes in *Vibrio campbellii*.

Importance

Wild isolates of bacterial type strains can yield important information about traits that vary within species. Here, we compare the recently sequenced isolate of *Vibrio campbellii* DS40M4 to the canonical lab type strain BB120 and examine several phenotypes that define this species, including quorum sensing, bioluminescence, and biofilm formation. Importantly, DS40M4 is naturally transformable with exogenous DNA, which allows for the rapid generation of mutants in a laboratory setting. By exploiting natural transformation, we genetically dissected the functions of BB120 quorum-sensing system homologs in the DS40M4 strain, including two-component signaling systems, transcriptional regulators, and small RNAs. Our results show important distinctions between the quorum-sensing circuits of these two strains that underscore the need to examine wild isolates alongside type strains.

Introduction

Quorum sensing is a form of cell-cell communication between bacteria in which individual cells synthesize and respond to signaling molecules called autoinducers. High concentrations of autoinducers trigger changes in gene expression among bacterial populations, resulting in group behaviors. Through this method of cell-cell signaling, bacteria control expression of genes involved in motility, toxin secretion, metabolism, and more (1). Quorum sensing has historically been heavily studied in marine *Vibrio* species, owing to easily observable behaviors such as bioluminescence and biofilm formation (2). *Vibrio campbellii* BB120 was one of the first *Vibrio* species to have its quorum-sensing circuit discovered (3–5). *V. campbellii* BB120 was historically called *Vibrio harveyi* BB120 (also known as strain ATCC BAA-1116) until it was recently reclassified (6). Although similar quorum-sensing system architectures have been established in other *Vibrios,* BB120 has remained a model organism for studying quorum sensing and signal transduction among Gram-negative bacteria.

In the *V. campbellii* BB120 quorum-sensing system, previous research has identified three membrane-bound histidine kinase receptors, CqsS, LuxPQ, and LuxN (Fig. 1) (7). These receptors bind to autoinducers CAI-1, AI-2, and HAI-1, respectively, which are constitutively produced by the autoinducer synthases, CqsA, LuxS, and LuxM, respectively. When cells are at low cell density (LCD), the local concentration of autoinducers produced by *V. campbellii* is insufficient to bind to the receptors, which results in the receptors functioning as kinases. As kinases, all three receptors phosphorylate LuxU, a phosphotransfer protein that transfers phosphate to the response regulator LuxO. Phosphorylated LuxO activates transcription of five small RNAs (sRNAs) termed quorum regulatory RNAs (Qrrs). The Qrrs posttranscriptionally repress production of the transcriptional regulator LuxR while activating expression of the transcriptional regulator AphA. The activation of AphA and repression of LuxR combinatorially regulates ~170 genes and produces individual behaviors in *V. campbellii*, including biofilm formation (Fig. 1) (8). As *V. campbellii* cells continue to grow and the local concentration of autoinducers produced by cells increases, the autoinducers bind to the receptors and change their kinase activity to act as phosphatases. This dephosphorylates LuxO, and the Qrrs are no longer expressed. The result at high cell density (HCD) is high expression of LuxR and no production of AphA. LuxR regulates >600 genes to produce group behaviors in *V. campbellii*, including activation of bioluminescence, type VI secretion (T6SS), and protease production, and repression of biofilm production and type III secretion (Fig. 1) (8, 9).

Natural transformation is the process by which bacteria uptake exogenous DNA and integrate it into their genome through homologous recombination. This process is well-studied in

Vibrio cholerae, which is capable of chitin-mediated natural transformation through the induction of its master competence regulator TfoX (10). By exploiting this process, researchers are able to make gene deletions, point mutations, unmarked mutations, and insertions using transformation (10–12). Importantly, multiple mutations can be generated simultaneously in *V. cholerae* through a technique termed MuGENT: multiplex genome editing by natural transformation (13, 14). Other *Vibrio* species, such *as Vibrio natriegens*, can successfully undergo chitin-independent transformation via overexpression of *V. cholerae* TfoX. Notably, the field has been unable to achieve natural transformation in BB120 with either method of transformation (15). The inability to rapidly generate defined mutations in BB120 has been a significant disadvantage, especially in comparison to other *Vibrio* species like *V. cholerae* that have more genetic tractability. BB120 is also a largely domesticated type strain, having been passaged in laboratory conditions for decades. Thus, the traits observed in BB120 likely vary compared to other *Vibrios* and wild isolates of *V. campbellii*.

Recently, we showed that natural transformation is achievable in two wild isolates of *V. campbellii*, DS40M4 and NBRC 15631, by inducing expression of TfoX (15). Furthermore, DS40M4 can transform at frequencies similar to *V. natriegens*, which has been reported as the strain with the highest transformation frequency thus far. While *V. campbellii* strains all contain homologs of the known competence genes, TfoX overexpression does not stimulate expression of these genes in BB120, unlike in the wild isolates. This suggests that BB120 may have lost regulation by TfoX due to domestication in laboratory conditions. We hypothesized that these environmental *V. campbellii* strains may exhibit differences in other behaviors such as growth and quorum sensing-controlled phenotypes. Here, we show that the recently sequenced environmental isolate *V. campbellii* DS40M4 (16–18) exhibits several advantages as a model organism compared to BB120. Using natural transformation to rapidly construct mutants, we tested differences in quorum sensing-controlled phenotypes between DS40M4 and BB120, including biofilm formation, T6SS-mediated cell killing, protease activity, and bioluminescence. Additionally, we demonstrate the power of MuGENT in DS40M4 by simultaneously introducing five mutations to a single strain in one transformation reaction. Altogether, our data show that while DS40M4 is similar to BB120 in the presence of specific genes, it has a distinct quorum-sensing circuit that produces different downstream behaviors.

Results

Comparison of growth, bioluminescence, and virulence-associated behaviors between V. campbellii *DS40M4 and BB120*

Because *V. campbellii* DS40M4 is a wild isolate, we hypothesized that DS40M4 possesses stronger virulence-associated characteristics compared to BB120. We first tested the growth rate of both strains and found that DS40M4 has a faster generation time of ~45 minutes, growing nearly twice as fast as BB120's doubling time of ~73 minutes (Fig. 2A). We next compared several virulence-associated behaviors between BB120 and DS40M4 and found differences between the two strains. First, DS40M4 exhibits stronger T6SS-dependent killing in competition assays with *Escherichia coli* (Fig. 2B). Interestingly, however, we found that BB120 shows significantly stronger biofilm formation, as well as nearly double the extracellular protease activity of DS40M4 (Fig. 2C, 2D). Finally, we examined BB120 and DS40M4 for bioluminescence activity. Unlike BB120, DS40M4 produces no bioluminescence at HCD (Fig. 2E). Comparison of the LuxCDABE protein sequences showed that DS40M4 only encodes a homolog of BB120 LuxB (no homologs of LuxCDAE) (Fig. 2F), and therefore lacks the genes required for bioluminescence.

Simultaneous construction of multiple mutations in DS40M4 using multiplex genome editing by natural transformation (MuGENT)

In several *Vibrio* species, natural transformation has been exploited as a means for construction of mutations in a highly efficient manner (14, 19, 20). Because *V. campbellii* DS40M4 exhibits high frequencies of natural transformation through ectopic over-expression of TfoX, we tested whether DS40M4 is capable of co-transformation of multiple transforming DNA substrates (tDNAs). Based on the literature on *V. cholerae*, we hypothesized that cells within the population that have the capacity to undergo natural transformation at high frequencies should be capable of taking up and integrating multiple tDNA products. To test this, we synthesized two linear tDNA products, each containing different antibiotic resistance cassettes: one targeting the *luxO* gene in DS40M4 to be replaced with a spectinomycin-resistance gene (*Spec*^{R}) and one targeting the *luxR* gene to be replaced with a trimethoprim-resistance gene (*Tm*^{R}). We added both tDNA substrates to cells induced for TfoX overexpression, and we plated with selection for Tm^R alone, $Spec^R$ alone, or both Tm^R and $Spec^R$. As expected, we isolated Tm^R and $Spec^R$

colonies each at a high efficiency (Fig. 3A). We isolated numerous colonies (4 x 10^5) when selecting for both antibiotics. Thus, we conclude that DS40M4 is capable of transformation of multiple DNA products.

In both *V. cholerae* and *V. natriegens*, multiple mutations can be introduced on the genome simultaneously using a process called MuGENT: multiplex genome editing by natural transformation (13, 20). This method utilizes one tDNA with a selectable antibiotic marker that is co-transformed with unselected tDNA substrates targeting other genes. This has been used to make concurrent unmarked deletions in up to four genes in a single transformation reaction in *V. natriegens* (13). Because *V. campbellii* DS40M4 is capable of efficiently transforming at least two tDNA products, we hypothesized that we could use MuGENT to introduce unmarked mutations onto the DS40M4 genome. We synthesized a linear tDNA product that targets the *luxB* gene in DS40M4 and replaces it with a Tm^R cassette to use as the selectable tDNA. The *luxB* gene was chosen because DS40M4 does not have a functional bioluminescence operon (Fig. 2E, 2F), and we predicted that deleting this gene should not greatly affect other cell processes. We explored the extent to which MuGENT can be used in DS40M4 and simultaneously examined the role of the Qrrs in DS40M4. We used MuGENT to construct strains with various combinations of Qrr deletions using five non-selectable tDNAs targeting the Qrr genes and one selectable tDNA targeting *luxB*. In a single MuGENT transformation experiment, 25% of Tm^R mutants contained one unselected genome edit, 22% contained two edits, 12.5% contained three, and 7.8% contained four unselected genome edits (Fig. 3B). We confirmed the presence of the unselected mutations using multiplex allele-specific colony (MASC)-PCR followed by sequencing (Fig. 3C) (21, 22). Although we were able to make various combinations of up to four unselected edits, none of the mutant colonies screened contained all five unselected deletions of the Qrr genes. We conclude that while *V. campbellii* DS40M4 has a high transformation frequency, the limit of one round of MuGENT in our testing was five mutations: four non-selected deletions and one selected deletion.

V. campbellii DS40M4 has an active quorum-sensing circuit that is distinct from BB120

We searched the DS40M4 genome for homologs of the proteins and sRNAs previously identified in the *V. campbellii* quorum-sensing system. DS40M4 encodes genes with high amino acid or nucleotide identity to all the components except for LuxM, for which there was no homolog in DS40M4 (Table 1).

To determine whether homologs of previously tested BB120 quorum-sensing sRNAs and proteins have similar functions in DS40M4, we generated numerous mutant strains, including Δ*cqsA*, Δ*luxS*, Δ*cqsA* Δ*luxS*, Δ*luxO*, Δ*luxR*, *luxO* D47E (a LuxO phosphomimic allele), in addition to every combination of *qrr* deletion (single or combined). We previously showed, using a $P_{luxCDABE}$-*gfp* reporter plasmid, that wild-type DS40M4 activates the *luxCDABE* promoter from BB120, and this is dependent on DS40M4 LuxR (15). We have since constructed a plasmid encoding the BB120 *luxCDABE* operon under control of its endogenous promoter (pCS38) for use in DS40M4, which enables us to monitor bioluminescence of various DS40M4 strains and assess LuxR regulation as a function of upstream quorum-sensing components.

DS40M4 produces and responds to CAI-1 and AI-2 but not HAI-1

DS40M4 lacks a LuxM homolog, which is the HAI-1 synthase in BB120 (Table 1). However, DS40M4 encodes a LuxN homolog that is 63% identical to BB120 LuxN (Fig. 4A, Table 1, Fig. S1A), which is the HAI-1 receptor that exhibits kinase activity in the absence of HAI-1 ligand and phosphatase activity when HAI-1 is bound. Curiously, there is high sequence conservation (91% amino acid identity) between the BB120 and DS40M4 LuxN proteins in the C-terminal receiver domain (amino acids 466-849), whereas the N-terminal region of BB120 LuxN (amino acids 1-465) that binds the HAI-1 autoinducer shares only 40% identity with DS40M4 LuxN (Fig. 4A, Fig. S1A). We wondered if this might suggest that the DS40M4 LuxN senses a different molecule than HAI-1, possibly produced by a different synthase. DS40M4 encodes close homologs of BB120 CqsS and LuxPQ, which bind CAI-1 and AI-2, respectively (98% and 99% amino acid identity, respectively; Table 1). We investigated the activity of the autoinducers produced by DS40M4 by collecting cell-free supernatant from DS40M4 and adding it to autoinducer-sensing reporter strains in the BB120 background in which a single autoinducer synthase is deleted. For example, a Δ*cqsA* BB120 strain is not producing CAI-1 and has a lower level of bioluminescence compared to wild-type (Fig. 4B). Addition of a supernatant containing CAI-1 such as BB120 supernatant results in an increase in bioluminescence (Fig. 4B). We observed that addition of DS40M4 supernatant increased bioluminescence in the AI-2 and CAI-1 BB120 sensing strains (Δ*luxS* and Δ*cqsA*, respectively), but did not affect bioluminescence in the HAI-1 sensing strain Δ*luxM. (*Fig. 4B). From these experiments, we conclude that DS40M4 produces AI-2 and CAI-1 molecules that can be sensed by BB120, but not an HAI-1 molecule.

We previously assessed the molecules sensed by DS40M4 receptors CqsS and LuxPQ (15). Our data showed that DS40M4 senses the AI-2 and CAI-1 molecules produced by BB120 but not BB120 HAI-1, even though DS40M4 encodes a LuxN homolog. From both sets of data

regarding autoinducers produced by BB120 and DS40M4, we conclude that DS40M4 does not produce or respond to HAI-1 under our lab conditions. However, our collective data did not address whether LuxN is functional. To determine whether DS40M4 LuxN is functional to act as a kinase, phosphatase, or both, we generated numerous mutants in the DS40M4 background and examined bioluminescence and biofilm formation at HCD. Bioluminescence is produced at HCD and biofilm formation is repressed at HCD. Based on the pathway characterized in BB120, if LuxN was functioning as a kinase, deletion of *luxN* would have a decreased pool of phosphorylated LuxO, decreased Qrr levels, increased LuxR levels, and finally increased bioluminescence and decreased biofilm formation. Conversely, if LuxN is functioning as a phosphatase, we predicted that deletion of *luxN* would decrease bioluminescence and increase biofilm production because there would be less phosphatase activity draining phosphate from LuxO. A *luxO* D47E mutant produces no bioluminescence and maximal biofilm formation because it is a phosphomimic of LuxO that acts as a constitutively phosphorylated LuxO (Fig. 4C, 4D).

For both phenotypes, the Δ*cqsA* Δ*luxS* mutant is significantly different from wild-type (Fig. 4C, 4D). Deletion of *luxS* or *cqsA* does not have a significant effect on bioluminescence (Fig. 4C). Conversely, deletion of *cqsA* but not *luxS* increases biofilm formation, which is analogous to what is observed for biofilm formation in *V. cholerae* (23) (Fig. 4D). Deletion of *luxR* does not maximize biofilm production, though the *luxO* D47E mutation does (Fig. 4D). We also noted that the Δ*cqsA* Δ*luxS* strain retains bioluminescence production more than 10-fold higher than the Δ*luxR* strain (Fig. 4C). Deletion of *luxN* decreases bioluminescence and increases biofilm formation compared to the Δ*cqsA* Δ*luxS* parent strain (Fig. 4C, 4D). Of note, the Δ*cqsA* Δ*luxS* Δ*luxN* strain has the highest level of biofilm formation, comparable to the *luxO* D47E strain. Deletion of *luxN* in the wild-type background does not impact biofilm formation (data not shown). This is likely because the other two receptors are acting as phosphatases in the wild-type strain at HCD. We conclude from these data that LuxN does not have kinase activity but has phosphatase activity acting on the LuxU-LuxO circuit. We suggest two possibilities: 1) LuxN functions as a phosphatase in the absence of a ligand, or 2) LuxN has phosphatase activity because it is bound to an unknown ligand.

<u>The Qrrs and LuxO in DS40M4 have different activities compared to BB120</u>

The wild-type DS40M4 strain exhibits a typical “U-shape” bioluminescence curve (in strains containing pCS38 expressing *luxCDABE*) in which bioluminescence is produced from the inoculum and is diluted by growth over time (Fig. 5A). As the cells grow to HCD, LuxR is

produced at higher levels, which in turn drives expression of the *luxCDABE* genes and bioluminescence is maximally produced at stationary phase. Because LuxR is a required activator of *luxCDABE*, a Δ*luxR* strain does not produce bioluminescence (Fig. 5A). DS40M4 encodes five Qrrs with high percent nucleotide identity and similar genome position compared to BB120 (Figure S2). Further, the Sigma-54 and LuxO binding sites identified in BB120 *qrr* promoters are conserved in DS40M4 (Fig. S2) (24). Thus, we predicted and observed that a DS40M4 strain lacking all of the *qrr1-5* genes does not inhibit LuxR production and is constitutively bright (Fig. 5A). The *luxO* D47E phosphomimic constitutively expresses Qrr sRNAs throughout the curve to inhibit LuxR production, resulting in no bioluminescence (Fig. 5A). Each of these phenotypes matches the analogous BB120 mutant phenotypes (24). However, the Δ*luxO* strain has a distinct difference. In BB120, a Δ*luxO* mutant strain is constitutively bright and is similar to the Δ*qrr1-5* strain because Δ*luxO* cannot express the Qrrs (25). Curiously, in DS40M4, the Δ*luxO* strain has a similar trend to wild-type (Fig. 5A), suggesting that in the absence of LuxO, this strain can still regulate bioluminescence production in a density-dependent manner. One possibility is that another functional LuxO is present in *V. campbellii*. Both BB120 and DS40M4 encode a second homolog with 49% identity to LuxO. However, deletion of the DS40M4 *luxO* homolog in both the wild-type and Δ*luxO* strains resulted in the same U-shaped curve (data not shown), indicating that this *luxO* homolog does not regulate bioluminescence. Given the epistatic relationship of the Qrrs to LuxO control of bioluminescence, we propose that regulation of bioluminescence is occurring via an additional regulatory circuit outside the LuxO quorum-sensing pathway that also converges on the Qrrs.

To further examine this result, we constructed strains containing different combinations of deletions of *qrr1-5* (Table S2). We first assessed the bioluminescence phenotype of each of the strains producing only a single Qrr, *e.g.*, *qrr1*+, *qrr2*+, *etc.* Surprisingly, these phenotypes also did not match previous data from BB120 (24). In analogous *qrr* mutant strains of BB120, the curve is still U-shaped but with increasing levels of bioluminescence depending on the Qrr gene expressed, such that the curves for each Qrr-expressing strain lie between the wild-type U-shaped curve and the Δ*qrr1-5* constitutively bright curve. Specifically, in BB120, expression of Qrr2 and Qrr4 alone exhibit the strongest effect on bioluminescence repression, followed by Qrr3, then Qrr1, and finally Qrr5, which has no effect when deleted because it is not expressed under tested conditions (24). Thus, in BB120, Qrr2/Qrr4>Qrr3>Qrr1>Qrr5 with regard to repression of bioluminescence. In contrast, in DS40M4, we observe that deletion of *qrrs* has a much different effect (Fig. 5B). A strain expressing only *qrr4* produces less bioluminescence than wild-type. Importantly, this occurs even at HCD, when the Qrrs are not expected to be

expressed based on data in BB120. The other strains exhibit varying phenotypes: *qrr1*+, *qrr*3+, and *qrr5*+ all have varying levels of bioluminescence production, each with a more flat-lined expression pattern across the growth curve and varying strengths such that Qrr4>Qrr5/Qrr3>Qrr1 (Fig. 5B). The *qrr2*+ strain appears to be the only one that follows the U-shape pattern observed in BB120. These data collectively indicate that expression of Qrrs is not controlled only by the quorum-sensing pathway with the exception of Qrr2. Because the *qrr2*+ strain exhibits near wild-type levels of bioluminescence throughout the curve, this suggests that Qrr2 is controlled solely by quorum sensing and has a strong repression effect on LuxR. However, expression of *luxO* D47E completely represses bioluminescence (Fig. 5A), suggesting that phosphorylated LuxO is epistatic to other regulatory inputs that activate bioluminescence.

The U-shape curve observed in the Δ*luxO* strain suggests that another quorum-sensing signal is controlling bioluminescence production. To test this, we constructed a Δ*luxO qrr4*+ strain. This strain produces a U-shaped curve similar to Δ*luxO* but produced less bioluminescence throughout the assay (Fig. 5C). This result confirms that Qrr4 expression is epistatic to LuxO. Further, another factor is likely altering expression of Qrr4 throughout the growth curve that also changes with cell density, as evidenced by the change in bioluminescence.

Virulence phenotypes are differentially regulated by quorum sensing in DS40M4 and BB120

Quorum sensing plays an important role in regulating several pathogenic behaviors in *Vibrio* strains. To assess the impact of quorum sensing on pathogenic behavior in DS40M4 and BB120, we compared several virulence phenotypes between different quorum-sensing mutants. We tested three different virulence phenotypes that are controlled by quorum sensing: type VI killing, exoprotease activity, and biofilm formation (26–28). BB120 exhibited stronger changes in type VI-dependent killing assays with quorum-sensing mutants (Fig. 6A). The LCD mutant strains, which are the *luxO* D47E strain and the Δ*luxR* strain, both showed increased type VI-dependent killing of *E. coli* compared to wild-type. However, DS40M4 quorum-sensing mutants showed no significant changes in type VI-dependent killing relative to the wild-type, suggesting that quorum sensing does not control this behavior in this strain (Fig. 6A). When we examined relative exoprotease activity between BB120 and DS40M4 strains, we observed analogous functions of the quorum-sensing proteins between the two strains. While BB120 exhibits stronger exoprotease activity than DS40M4, exoprotease activity significantly drops in LCD mutants, suggesting this behavior is dependent on LuxR in both BB120 and DS40M4 (Figure

6B). Comparing biofilm formation between DS40M4 and BB120 mutants showed that LCD mutants exhibit increased biofilm formation compared to the wild-type parent strain (Figure 6C). Interestingly, however, while BB120 overall has significantly stronger biofilm formation than DS40M4, quorum sensing appears to regulate biofilm formation more strongly in DS40M4 than in BB120. From these experiments, we conclude that quorum sensing controls protease production and biofilm formation in both BB120 and DS40M4, whereas type VI killing is only regulated by quorum sensing in BB120.

dRNA-seq identifies the quorum-sensing regulon and transcriptional start sites of DS40M4 genes

To facilitate the use of DS40M4 as a model quorum-sensing strain, we defined the genes regulated by quorum sensing. Using RNA-seq, we compared gene expression of wild-type and Δ*luxR* cultures grown to OD_{600} = 1.0, which is the point at which bioluminescence is maximal (Fig. 5). LuxR regulates 90 genes >2-fold ($p > 0.05$, Table S1), including those involved in metabolism, cyclic di-GMP synthesis, transport, and transcriptional regulation. This is a smaller regulon than those observed in other vibrios, including BB120 in which LuxR regulates >400 genes (29, 30). Certain genes that are regulated by LuxR in other vibrios, such as type VI secretion genes, are not regulated by LuxR in DS40M4. Further, the fold-change in gene activation and repression by LuxR is smaller. For example, the type III secretion operons in DS40M4 are all repressed <2-fold by LuxR, whereas these are repressed >10-fold in BB120.

To verify the results of the RNA-seq analysis, we performed qRT-PCR on wild-type, Δ*luxR*, and Δ*qrr1-5* DS40M4 strains to examine the transcript levels for *luxR*, *aphA*, and type III and type VI secretion genes. RNA samples were collected from these three strains at LCD (OD_{600} = 0.1), HCD (OD_{600} = 1.0), and late stationary phase (OD_{600} = 3.25), and measured by qRT-PCR. Our results confirm that *luxR* is expressed at the highest levels late stationary phase and is repressed by *qrr1-5* at LCD (Figure 7A). Similar to what is observed in BB120, *aphA* and the type III secretion gene *exsB* are more highly expressed at LCD, repressed by LuxR, and activated by *qrr1-5* (Fig. 7B, 7C). The type VI secretion gene *tssC* is remarkably more highly activated at late stationary phase (Fig. 7D). This result agrees with the type VI killing assay in which quorum sensing mutants were not different than wild-type. Together, our qRT-PCR results confirmed our RNA-seq results. We conclude that the LuxR regulon in DS40M4 is smaller than that of LuxR in BB120, and the fold-change of regulation is reduced in DS40M4.

In addition to establishing the LuxR regulon in DS40M4, we also used differential RNA-seq (dRNA-seq) to determine the transcription start sites for all the genes expressed in

DS40M4, both in wild-type and Δ*luxR* strains. Three examples are shown in Figure 7E, in which the transcription start sites determined by dRNA-seq are shown for *luxR*, *exsB* (type III secretion), and *tssABC* (type VI secretion). This transcriptomic experiment provides critical data for future genetic and mechanistic studies of quorum-sensing gene expression.

Discussion

V. campbellii BB120 has historically served as the primary model strain for quorum-sensing experiments in *Vibrio* species. BB120 was isolated as a conjugation-proficient mutant of parent strain BB7 that arose after multiple cycles of conjugation and laboratory passaging (Bonnie Bassler, personal communication). It is perhaps not surprising that the wild isolate DS40M4 strain isolated by Margo Haygood (18) exhibits different physiological and functional characteristics compared to BB120. DS40M4 grows at a faster rate and exhibits increased T6SS-induced killing of *E. coli* cells. Interestingly, however, we found that BB120 exhibits much stronger biofilm formation than DS40M4, a trait often lost in laboratory conditions (31–33), as well as an increase in exoprotease production (34). In addition, DS40M4 is one of many dark (non-bioluminescent) *Vibrio campbellii* isolates that contain lesions in the *lux* locus that abrogate bioluminescence production (35). As an environmental isolate, DS40M4 likely serves as a better model for comparing behaviors of *V. campbellii* to *Vibrio* strains in their native marine environment. One such behavior is the type VI secretion activity of DS40M4. It will be informative to assess the effects of increased type VI secretion and growth rate on virulence in host systems in future studies, as well as other virulence-associated characteristics such as type III secretion and motility.

Unfortunately, although BB120 still remains a core model strain for *Vibrio* studies, it is one of several *Vibrio* strains that is not capable of natural transformation, at least not under any conditions we have tested (15). Thus, making mutations in BB120 is laborious and requires construction of suicide plasmids and the use of counter-selection and colony screening. Here we expanded upon our previous study of natural transformation in DS40M4 (15) to show the power of natural transformation for constructing up to four unmarked mutations simultaneously. The Qrr genes in the quorum-sensing circuit are only one example of a gene set for which MuGENT is useful in studying combinatorial mutant phenotypes. The ease with which mutants are constructed in DS40M4 allowed us to quickly generate deletion mutants of several core quorum-sensing genes. Our results from assessing the autoinducers produced and detected by DS40M4 suggest that there is likely another arm of the circuit. DS40M4 shares the AI-2/CAI-1

pathway of BB120, but it lacks a LuxM (HAI-1 synthase) homolog, and its LuxN (HAI-1 receptor) homolog is only 63% identical. Although the DS40M4 LuxN homolog cannot sense HAI-1 from BB120, our data suggest that LuxN has phosphatase activity that acts in the quorum-sensing circuit. While the biochemical activity of DS40M4 LuxN remains to be tested, one possibility is that LuxN has more phosphatase activity than kinase activity, thus it is constitutively dephosphorylating LuxU. Another possibility is that DS40M4 LuxN senses an unidentified autoinducer produced by a different synthase than LuxM, thus resulting in phosphatase activity at HCD as has been shown for BB120 LuxN. Genetic screens will likely differentiate these two possibilities.

Several of the recently identified quorum-sensing receptor proteins in *V. cholerae* have not yet been characterized in BB120. CqsR and VpsS are additional histidine sensor kinases in *V. cholerae* that phosphorylate LuxU (36). The ligands for these receptors are unknown (37). BB120 encodes homologs to both *V. cholerae* CqsR and VpsS with a percent identity of 54.76% and 50.35%, respectively (Table 2). Conversely, DS40M4 appears to only encode a clear CqsR homolog. Although we identified numerous homologs of VpsS in DS40M4, each has incomplete coverage and low identity. The amino acid identity of these homologs lies in the kinase/receiver domain, and thus these homologs are likely other putative sensor kinases but not necessarily VpsS-like proteins nor connected to quorum sensing (Table 2). Another quorum-sensing system in *V. cholerae* has been identified in which the molecule DPO (3,5-dimethylpyrazin-2-ol, synthesized by threonine dehydrogenase) is bound by transcription factor VqmA (38). VqmA-DPO activates expression of a sRNA (VqmR) that represses biofilm formation. A homolog of VqmA is present in both BB120 and DS40M4 (Table 2), and a putative VqmR lies directly upstream of these *vqmA* genes. Both BB120 and DS40M4 encode Tdh, which is not surprising given its role in metabolism (Table 2). However, the production of DPO, the function of VqmA and VqmR, and any connection to downstream genes still remains to be tested in most *Vibrios*, including BB120 and DS40M4. Based on our data and the recent identification of novel autoinducers/receptors in *V. cholerae* (36, 38), it is very possible that there are other quorum-sensing components that act in parallel or integrate into the known circuit that have yet to be identified in various *Vibrio* species.

Our data also suggest that DS40M4 contains a regulator that converges on the quorum-sensing circuit at the Qrrs. Contrary to BB120, deletion of *luxO* in DS40M4 does not result in maximal quorum sensing (monitored via bioluminescence production). The Δ*luxO* strain is quite similar to wild-type DS40M4, whereas the Δ*qrr*1-5 mutant has maximal bioluminescence at all cell densities. Further complicating quorum-sensing regulation, our data also show that when

qrr4 is the only *qrr* gene remaining in DS40M4, cells have constitutively low bioluminescence levels. Interestingly, deletion of LuxO in the *qrr4*+ background is not sufficient to fully maximize quorum sensing, and bioluminescence still shows a cell density-dependent response. We propose that LuxO is not the sole regulator for the Qrrs, and that an additional regulator acts to influence Qrr expression in DS40M4. Although DS40M4 and BB120 have an additional LuxO homolog, the transcript levels of these genes are very low in both strains, and deletion of the homolog in the DS40M4 strain did not result in a constitutively bright strain. Genetic screens will likely uncover any additional regulator(s) of the Qrrs.

Previous studies of quorum sensing in *V. harveyi* have typically been performed in BB120, and quorum-sensing models for this strain presumably apply to other *V. harveyi/campbellii* strains. However, while it is understood and accepted that strains of the same bacterial species can vary widely in nature, it isn't often investigated how the canonical models diverge amongst these strains. Although BB120 and DS40M4 share an average nucleotide identify of 98.02% (16), we have shown that these two strains differ widely from one another in natural transformation, quorum-sensing pathways, and virulence phenotypes. It is important to consider strain to strain variations and how bacteria in the environment may differ from the models established from laboratory strains. Here we have shown that the environmental isolate DS40M4 may serve as a powerful and relevant model strain when studying behaviors in *V. campbellii*.

Materials and Methods

Bacterial strains and media

All bacterial strains and plasmids are listed in Tables S2 and S3. *V. campbellii* strains were grown at 30°C on Luria marine (LM) medium (Lysogeny broth supplemented with an additional 10 g NaCl per L). Instant ocean water (IOW) medium was used in the chitin-independent transformations; it consists of Instant Ocean sea salts (Aquarium Systems, Inc.) diluted in sterile water (2X = 28 g/l). Transformations were outgrown in LBv2 (Lysogeny Broth medium supplemented with additional 200 mM NaCl, 23.14 mM $MgCl_2$, and 4.2 mM KCl). When necessary, strains were supplemented with kanamycin (100 µg/ml), spectinomycin (200 µg/ml), gentamicin (100 µg/ml), or trimethoprim (10 µg/ml). Plasmids were transferred from *E. coli* to *Vibrio* strains by conjugation on LB plates. Exconjugants were selected on LM plates with polymyxin B at 50 U/ml and the appropriate selective antibiotic.

Construction of linear tDNAs

All PCR products were synthesized using Phusion HF polymerase (New England Biolabs). Sequencing of constructs and strains was performed at Eurofins Scientific. Cloning procedures and related protocols are available upon request. Oligonucleotides used in the study are listed in Table S4. Linear tDNAs were generated by splicing-by-overlap extension (SOE) PCR as previously described (39).

Natural Transformation

Chitin-independent transformations were performed following the protocol established in Dalia *et al*. 2017 (13). Transformation frequency was calculated as the number of antibiotic-resistant colonies divided by viable cells. Following natural transformation, strains containing the correct target mutation were identified via colony PCR with a forward and reverse detection primer. Following MuGENT, colonies were screened for integration of unselected genome edits via MASC-PCR as described previously (20). Detection primers are listed in Table S3.

Bioluminescence assays and growth curves

For the bioluminescence growth assays, overnight cultures were back-diluted to an OD_{600} = 0.0005 in 25 ml LM with selective antibiotics as required and incubated at 30°C shaking at 275 RPM. The OD_{600} was recorded every 45 minutes using a spectrophotometer, and bioluminescence was measured in black-welled clear-bottom 96-well plates using the BioTek Cytation 3 Plate Reader (gain set at 160). For endpoint bioluminescence assays, strains were back-diluted to 1:1,000 in 5 ml LM with selective antibiotics as required and incubated at 30°C shaking at 275 RPM for 7 h. 200 ul of the culture was transferred to a black-welled clear-bottom 96-well plate and the OD_{600} and bioluminescence were measured using the BioTek Cytation 3 Plate Reader (gain 160). For growth assays, overnight cultures were back-diluted 1:1,000 in 200 µl LM in a 96-well plate, and incubated at 30°C shaking in the BioTek Cytation 3 Plate Reader. OD_{600} was recorded every 30 minutes in the plate reader for a total of 24 hours.

Autoinducer Assays

Overnight cultures of supernatant strains were back-diluted 1:100 in fresh media and incubated at 30°C shaking at 275 RPM until the OD_{600} ~2.0. Cultures were centrifuged to pellet cells at 16,200 x g, supernatants were filtered through 0.22-µm filters, and these were added to fresh medium at 20% final concentration. Cells from strains to be assayed in the

presence of supernatants were added to these supplemented media at a 1:5,000 dilution of the overnight culture and incubated shaking at 30°C at 275 RPM overnight. Bioluminescence and OD_{600} were measured in black-welled clear-bottom 96-well plates using the BioTek Cytation 3 Plate Reader.

Extracellular protease activity assay

Extracellular protease activity was determined as previously described (40). Briefly, all strains were back-diluted 1:1,000 in LM medium and grown at 30°C shaking at 275 RPM for 9 h. The culture OD_{600} was measured, and the strains were collected by centrifugation at 3700 x *g* for 10 min. The supernatants of each strain were filtered through 0.22 µm filters and 1 ml of filtered supernatant was mixed with 1 ml phosphate buffer saline (PBS, pH 7.2) and 10 mg of hide powder azure (HPA). These mixtures were incubated at 37°C while shaking at 275 RPM for 2 h, and the reactions were stopped by adding 1 ml 10% trichloroacetic acid (TCA). Total protease activity was measured at 600 nm on a spectrophotometer and then normalized for each strain by dividing by the culture OD_{600}.

Biofilm formation assay

Biofilm formation was measured as previously described (41). Overnight cultures of strains grown in seawater tryptone (SWT) medium were diluted to OD_{600} = 0.005 in SWT and grown statically in six replicates in 96-well microtiter plates at 30°C for 24 h. The OD_{600} of the strains in the plate were measured, and the plates were rinsed with deionized water. 0.1% crystal violet was added to each well, and the plate was subsequently rinsed with deionized water. The crystal violet-stained biofilms were then solubilized with 33% acetic acid and measured at 590 nm using the BioTek Cytation 3 Plate Reader and normalized to the OD_{600}.

Type VI secretion competition assay

Type VI killing was measured using a competition assay as previously described (42). Predator strains (*V. campbellii*) were grown in LM medium overnight at 30°C, while the prey strain (*E. coli* S17-1λpir) was grown in LB at 37°C. Predator strains were diluted 1:20 and prey strains were diluted 1:40 and grown until they reached an OD_{600} between 0.6-1.2. Cells were harvested by centrifugation at 3,700 x *g* for 10 min, and then resuspended in fresh LB to reach an OD_{600} = 10. Predator and prey strains were mixed at a ratio of 1:1, and 5 µl of each mixture was spotted onto a piece of sterile filter paper fitted to an LB plate. The competition was carried out at 30°C for 4 h, and then each filter paper was moved to 0.5 ml of LB and vortexed to

resuspend the cells. These suspensions were serially diluted and plated on prey-selective plates (LB+trimethoprim$_{10}$). Plates were incubated at 37°C until colonies were visible, then colonies were counted to determine CFU of the surviving prey.

dRNA-Seq analysis

cDNA libraries were constructed as described previously (43) by Vertis Biotechnology AG (Freising, Germany) and sequenced using an Illumina NextSeq 500 machine in single-read mode (75 bp read length). The raw, demultiplexed reads and coverage files have been deposited in the National Center for Biotechnology Information Gene Expression Omnibus with accession code GSE147616.

RNA extraction and quantitative reverse transcriptase real-time PCR (qRT-PCR)

Strains were inoculated in 5 ml LM and grown overnight shaking at 30°C at 275 RPM. Each strain was back-diluted 1:1,000 in LM and grown shaking at 30°C at 275 RPM until they reached an OD_{600} = 0.1, 1.0, or 3.25. Cells were collected by centrifugation at 3,700 RPM at 4°C for 10 min, the supernatant was removed, and the cell pellets were flash frozen in liquid N_2 and stored at -80°C. RNA was isolated from pellets using a TRIzol/chloroform extraction protocol as described (44) and treated with DNase via the DNA-free™ DNA Removal Kit (Invitrogen).

qRT-PCR was used to quantify transcript levels of specific quorum sensing-controlled genes in DS40M4 and was performed using the SensiFast SYBR Hi-ROX One-Step Kit (Bioline) according to the manufacturer's guidelines. Primers were designed to have the following parameters: amplicon size of 100 bp, primer size of 20-28 nt, and melting temperature of 55-60°C. All reactions were performed using a LightCycler 4800 II (Roche) with 0.4 µM of each primer and 5 ng of template RNA (10 µl total volume). All qRT-PCR experiments were normalized to *hfq* expression and were performed with 2-4 biological replicates and 2 technical replicates.

Acknowledgements

We thank Victoria Lydick for excellent technical support, Ryan Chaparian for assistance with sequence alignments, and Konrad Förstner for support with the dRNA-Seq analysis. We would also like to acknowledge the IU Arts and Sciences Undergraduate Research Experience (ASURE) for encouraging and preparing the undergraduate researchers (LG and AL) as well as Charlotte & Jim Griffin for their support of the ASURE program. This work was supported by

the National Institutes of Health grant R35GM124698 to JVK. KP acknowledges funding by the European Research Council (StG-758212) and DFG (EXC 2051, Project 390713860).

References

1. **Rutherford ST**, **Bassler BL**. 2012. Bacterial quorum sensing: Its role in virulence and possibilities for its control. Cold Spring Harb Perspect Med **2**:1–25.
2. **Bassler BL**, **Greenberg EP**, **Stevens AM**. 1997. Cross-species induction of luminescence in the quorum-sensing bacterium *Vibrio harveyi*. J Bacteriol **179**:4043 LP – 4045.
3. **Freeman JA**, **Lilley BN**, **Bassler BL**. 2000. A genetic analysis of the functions of LuxN: A two-component hybrid sensor kinase that regulates quorum sensing in *Vibrio harveyi*. Mol Microbiol **35**:139–149.
4. **Bassler BL**, **Wright M**, **Silverman MR**. 1994. Sequence and function of LuxO, a negative regulator of luminescence in *Vibrio harveyi*. Mol Microbiol **12**:403–412.
5. **Bassler BL**, **Wright M**, **Showalter RE**, **Silverman MR**. 1993. Intercellular signalling in *Vibrio harveyi*: sequence and function of genes regulating expression of luminescence. Mol Microbiol **9**:773–786.
6. **Lin B**, **Wang Z**, **Malanoski AP**, **O'Grady EA**, **Wimpee CF**, **Vuddhakul V**, **Alves N**, **Thompson FL**, **Gomez-Gil B**, **Vora GJ**. 2010. Comparative genomic analyses identify the *Vibrio harveyi* genome sequenced strains BAA-1116 and HY01 as *Vibrio campbellii*. Environ Microbiol Rep **2**:81–89.
7. **Jung SA**, **Hawver LA**, **Ng WL**. 2016. Parallel quorum sensing signaling pathways in *Vibrio cholerae*. Curr Genet **62**:255–260.
8. **Van Kessel JC**, **Rutherford ST**, **Shao Y**, **Utria AF**, **Bassler BL**. 2013. Individual and combined roles of the master regulators AphA and LuxR in control of the *Vibrio harveyi* quorum-sensing regulon. J Bacteriol **195**:436–443.
9. **Bagert JD**, **Van Kessel JC**, **Sweredoski MJ**, **Feng L**, **Hess S**, **Bassler BL**, **Tirrell DA**. 2016. Time-resolved proteomic analysis of quorum sensing in *Vibrio harveyi*. Chem Sci **7**:1797–1806.
10. **Meibom KL**, **Blokesch M**, **Dolganov NA**, **Wu CY**, **Schoolnik GK**. 2005. Microbiology: Chitin induces natural competence in *Vibrio cholerae*. Science (80-) **310**:1824–1827.
11. **Yamamoto S**, **Izumiya H**, **Mitobe J**, **Morita M**, **Arakawa E**, **Ohnishi M**, **Watanabe H**. 2011. Identification of a chitin-induced small RNA that regulates translation of the *tfoX*

gene, encoding a positive regulator of natural competence in *Vibrio cholerae*. J Bacteriol **193**:1953–1965.

12. **Sun Y**, **Bernardy EE**, **Hammer BK**, **Miyashiro T**. 2013. Competence and natural transformation in vibrios. Mol Microbiol **89**:583–595.
13. **Dalia TN**, **Hayes CA**, **Stolyar S**, **Marx CJ**, **McKinlay JB**, **Dalia AB**. 2017. Multiplex Genome Editing by Natural Transformation (MuGENT) for Synthetic Biology in *Vibrio natriegens*. ACS Synth Biol **6**:1650–1655.
14. **Dalia AB**. 2018. Natural Cotransformation and Multiplex Genome Editing by Natural Transformation (MuGENT) of *Vibrio cholerae*, p. 53–64. *In* Sikora, AE (ed.), *Vibrio Cholerae*: Methods and Protocols. Springer New York, New York, NY.
15. **Simpson CA**, **Podicheti R**, **Rusch DB**, **Dalia AB**, **van Kessel JC**. 2019. Diversity in Natural Transformation Frequencies and Regulation across *Vibrio* Species. MBio **10**:1–16.
16. **Colston SM**, **Hervey WJ**, **Horne WC**, **Haygood MG**, **Petersen BD**, **van Kessel JC**, **Vora GJ**. 2019. Complete Genome Sequence of *Vibrio campbellii* DS40M4 . Microbiol Resour Announc **8**:1–2.
17. **Sandy M**, **Han A**, **Blunt J**, **Munro M**, **Haygood M**, **Butler A**. 2010. Vanchrobactin and anguibactin siderophores produced by *Vibrio* sp. DS40M4. J Nat Prod **73**:1038–1043.
18. **Haygood MG**, **Holt PD**, **Butler A**. 1993. Aerobactin production by a planktonic marine *Vibrio* sp. Limnol Oceanogr **38**:1091–1097.
19. **Chimalapati S**, **de Souza Santos M**, **Servage K**, **De Nisco NJ**, **Dalia AB**, **Orth K**. 2018. Natural Transformation in *Vibrio parahaemolyticus*: a Rapid Method To Create Genetic Deletions. J Bacteriol **200**:e00032-18.
20. **Dalia AB**, **McDonough E**, **Camilli A**. 2014. Multiplex genome editing by natural transformation. Proc Natl Acad Sci **111**:8937–8942.
21. **Wang HH**, **Church GM**. 2011. Multiplexed genome engineering and genotyping methods: Applications for synthetic biology and metabolic engineering. Methods in Enzymology, 1st ed. Elsevier Inc.
22. **Isaacs FJ**, **Carr PA**, **Wang HH**, **Lajoie MJ**, **Sterling B**, **Kraal L**, **Tolonen AC**, **Gianoulis TA**, **Goodman DB**, **Reppas NB**, **Emig CJ**, **Bang D**, **Hwang SJ**, **Jewett MC**, **Jacobson JM**, **Church GM**. 2011. Precise Manipulation of Chromosomes in Vivo Enables Genome-Wide Codon Replacement. Science (80-) **333**:348 LP – 353.
23. **Bridges AA**, **Bassler BL**. 2019. The intragenus and interspecies quorum-sensing autoinducers exert distinct control over *Vibrio cholerae* biofilm formation and dispersal.

PLoS Biol **17**:1–28.

24. **Tu KC**, **Bassler BL**. 2007. Multiple small RNAs act additively to integrate sensory information and control quorum sensing in *Vibrio harveyi*. Genes Dev **21**:221–233.
25. **Chaparian RR**, **Tran MLN**, **Miller Conrad LC**, **Rusch DB**, **van Kessel JC**. 2019. Global H-NS counter-silencing by LuxR activates quorum sensing gene expression. Nucleic Acids Res 1–13.
26. **Shao Y**, **Bassler BL**. 2014. Quorum regulatory small RNAs repress type VI secretion in *Vibrio cholerae*. Mol Microbiol2014/04/24. **92**:921–930.
27. **Anetzberger C**, **Reiger M**, **Fekete A**, **Schell U**, **Stambrau N**, **Plener L**, **Kopka J**, **Schmitt-Kopplin P**, **Hilbi H**, **Jung K**. 2012. Autoinducers Act as Biological Timers in *Vibrio harveyi*. PLoS One **7**.
28. **Waters CM**, **Lu W**, **Rabinowitz JD**, **Bassler BL**. 2008. Quorum sensing controls biofilm formation in *Vibrio cholerae* through modulation of cyclic Di-GMP levels and repression of vpsT. J Bacteriol **190**:2527–2536.
29. **Van Kessel JC**, **Rutherford ST**, **Shao Y**, **Utria AF**, **Bassler BL**. 2013. Individual and combined roles of the master regulators apha and luxr in control of the *Vibrio harveyi* quorum-sensing regulon. J Bacteriol **195**:436–443.
30. **Chaparian RR**, **Olney SG**, **Hustmyer CM**, **Rowe-Magnus DA**, **van Kessel JC**. 2016. Integration host factor and LuxR synergistically bind DNA to coactivate quorum-sensing genes in *Vibrio harveyi*. Mol Microbiol **101**:823–840.
31. **White AP**, **Surette MG**. 2006. Comparative genetics of the rdar morphotype in *Salmonella*. J Bacteriol **188**:8395–8406.
32. **Davidson CJ**, **White AP**, **Surette MG**. 2008. Evolutionary loss of the rdar morphotype in *Salmonella* as a result of high mutation rates during laboratory passage. ISME J **2**:293–307.
33. **McLoon AL**, **Guttenplan SB**, **Kearns DB**, **Kolter R**, **Losick R**. 2011. Tracing the domestication of a biofilm-forming bacterium. J Bacteriol **193**:2027–2034.
34. **Steensels J**, **Gallone B**, **Voordeckers K**, **Verstrepen KJ**. 2019. Domestication of Industrial Microbes. Curr Biol **29**:R381–R393.
35. **O'Grady EA**, **Wimpee CF**. 2008. Mutations in the *lux* operon of natural dark mutants in the genus *Vibrio*. Appl Environ Microbiol **74**:61–66.
36. **Jung SA**, **Chapman CA**, **Ng WL**. 2015. Quadruple Quorum-Sensing Inputs Control *Vibrio cholerae* Virulence and Maintain System Robustness. PLoS Pathog **11**:1–19.
37. **Watve S**, **Barrasso K**, **Jung SA**, **Davis KJ**, **Hawver LA**, **Khataokar A**, **Palaganas RG**,

Neiditch MB, **Perez LJ**, **Ng W-L**. 2020. Parallel quorum-sensing system in *Vibrio cholerae* prevents signal interference inside the host. PLOS Pathog **16**:e1008313.

38. **Papenfort K**, **Silpe JE**, **Schramma KR**, **Cong J-P**, **Seyedsayamdost MR**, **Bassler BL**. 2017. A *Vibrio cholerae* autoinducer–receptor pair that controls biofilm formation. Nat Chem Biol **13**:551–557.

39. **Dalia AB**, **Lazinski DW**, **Camilli A**. 2014. Identification of a membrane-bound transcriptional regulator that links chitin and natural competence in *Vibrio cholerae*. MBio **5**.

40. **Gu D**, **Guo M**, **Yang M**, **Zhang Y**, **Zhou X**, **Wang Q**. 2016. A σ^E-Mediated Temperature Gauge Controls a Switch from LuxR-Mediated Virulence Gene Expression to Thermal Stress Adaptation in *Vibrio alginolyticus*. PLoS Pathog **12**:1–31.

41. **O'Toole GA**. 2010. Microtiter dish Biofilm formation assay. J Vis Exp 10–11.

42. **Hachani A**, **Lossi NS**, **Filloux A**. 2013. A visual assay to monitor T6SS-mediated bacterial competition. J Vis Exp e50103.

43. **Papenfort K**, **Förstner KU**, **Cong JP**, **Sharma CM**, **Bassler BL**. 2015. Differential RNA-seq of *Vibrio cholerae* identifies the VqmR small RNA as a regulator of biofilm formation. Proc Natl Acad Sci U S A **112**:E766–E775.

44. **Rutherford ST**, **van Kessel JC**, **Shao Y**, **Bassler BL**. 2011. AphA and LuxR/HapR reciprocally control quorum sensing in vibrios. Genes Dev **25**:397–408.

698 **Table 1. DS40M4 homologs of established BB120 quorum-sensing proteins.**

699

Gene name	Amino acid identity	Query Cover	BB120 locus tag[a]	DS40M4 locus tag[b]
cqsA	97.96%	100%	VIBHAR_06088	DSB67_15960
cqsS	98.83%	100%	VIBHAR_06089	DSB67_15965
luxM	N/A	N/A	VIBHAR_02765	N/A
luxN	63.23%	99%	VIBHAR_02766	DSB67_09895
luxP	97.26%	100%	VIBHAR_05351	DSB67_22210
luxQ	98.37%	100%	VIBHAR_05352	DSB67_22215
luxS	98.84%	100%	VIBHAR_03484	DSB67_12735
luxU	96.49%	100%	VIBHAR_02958	DSB67_10605
luxO	98.34%	100%	VIBHAR_02959	DSB67_10610
luxR	99.51%	100%	VIBHAR_03459	DSB67_12620
aphA	99.44%	100%	VIBHAR_00046	DSB67_14070

700 a. Accession numbers: CP000789, CP000790, CP000791.

701 b. Accession numbers: CP030788, CP030789, CP030790

702

703 **Table 2. BB120 and DS40M4 homologs of *V. cholerae* quorum-sensing receptor proteins.**

704

	BB120[a]			DS40M4[b]		
Gene name	Amino acid identity to *V. cholerae*	Query Cover	Locus tag	Amino acid identity to *V. cholerae*	Query Cover	Locus tag
vqmA	64.5%	92%	VIBHAR_07094	64.5%	92%	DSB67_18870
Tdh	91.84%	100%	VIBHAR_05001	91.55%	100%	DSB67_20895
cqsR	54.76%	98%	VIBHAR_01620	55.03%	98%	DSB67_05165
vpsS	50.35%	98%	VIBHAR_02306	65% 69% 70% 72% 69% 67% 65%	39.37% 36.50% 39.49% 31.11% 37.06% 36.16% 40.45%	DSB67_09490 DSB67_07055 DSB67_07080 DSB67_12445 DSB67_12965 LuxQ DSB67_19025

705 a. Accession numbers: CP000789, CP000790, CP000791.

706 **b.** Accession numbers: CP030788, CP030789, CP030790.

707

Figure legends

Figure 1: Model for quorum-sensing regulation in *V. campbellii*. The autoinducers CAI-1, HAI-1, AI-2, are produced by autoinducer synthases CqsA, LuxM, and LuxS, respectively. At LCD, autoinducers are at low concentrations, resulting in the receptors acting as kinases. The three receptors phosphorylate LuxU (phosphorelay protein), which transfers the phosphate to LuxO. Phosphorylated LuxO activates *qrr* expression through Sigma-54. The Qrrs together with Hfq bind to the *aphA* and *luxR* mRNAs, and AphA is expressed and LuxR production is minimal. The combination of AphA and LuxR protein levels leads to LCD behaviors, such as type III secretion and biofilm formation. As autoinducers accumulate at HCD, the receptors bind autoinducers and in this state act as phosphatases. De-phosphorylated LuxO does not activate the *qrr* genes, thus leading to maximal LuxR and absence of AphA. This ultimately leads to HCD behaviors such as bioluminescence, proteolysis, and type VI secretion. Image created with BioRender.com.

Figure 2: Comparison of growth and virulence-associated phenotypes between BB120 and DS40M4. (A) Growth curve comparing growth rates between BB120 and DS40M4 in LM media. (B) Survival of *E. coli* cells in T6SS-dependent killing assays (n = 9). (C) Biofilm formation measured by crystal violet staining (OD_{595}) normalized to cell density (OD_{600}) (n = 6). (D) Exoprotease activity measured by HPA digestion and normalized to cell density (OD_{600}) (n = 3). (E) Bioluminescence production normalized to cell density (OD_{600}) (n = 4). (F) Diagram indicating the presence of the genes encoding LuxCDABE in BB120 and in DS40M4. For all panels, unpaired, two-tailed t-tests were performed on log-transformed data.

Figure 3. **MuGENT enables deletion of Qrr sRNAs in combinations of up to four unselected mutations.** (A) Co-transformation of linear tDNAs targeting *luxO* (*luxO::spec*^{R}) and *luxR* (*luxR::TM*^{R}). Transformation frequencies are shown for colonies selected on media containing spectinomycin ($Spec^R$), trimethoprim (TM^R), or both ($Spec^R$, TM^R). (B) Frequency of recovery of the selectable *luxB* deletion alone or in combination with one, two, three, or four *qrr* deletions using MuGENT in DS40M4. (C) Representative agarose gel of 24 MASC-PCR products from transformations targeting all five *qrr* genes *(qrr1-5)* and *luxB* in DS40M4. The presence of a band indicates that the gene has been deleted in that colony.

741 **Figure 4**. ***V. campbellii*** **DS40M4 produces and responds to CAI-1 and AI-2 autoinducers,**
742 **but not AI-1.** (A) Diagram of the predicted structure of the DS40M4 LuxN monomer. The
743 conserved C-terminal domain is colored purple, and the N-terminal region that is not conserved
744 is colored orange. Image created with BioRender.com. (B) Bioluminescence production
745 normalized to cell density (OD_{600}) for strains in which supernatants from the indicated strains
746 were added to BB120 strains. (C) Bioluminescence production normalized to cell density
747 (OD_{600}). (D) Biofilm formation measured by crystal violet staining (OD_{595}) normalized to cell
748 density (OD_{600}). For panels B, C, and D, different letters indicate significant differences in 2-
749 way ANOVA of log-transformed data followed by Tukey's multiple comparison's test ($n = 3$ or n
750 $= 4$, $p < 0.05$). For panel B, statistical comparisons were performed comparing the effects of the
751 three supernatant conditions for each reporter strain; data were not compared between reporter
752 strains.
753
754 **Figure 5**. **Quorum sensing regulation of bioluminescence in DS40M4 is distinct from**
755 **BB120.** For all panels A, B, and C, bioluminescence production is shown normalized to cell
756 density (OD_{600}) during a growth curve. A strain expressing only a single *qrr* is labeled with a '+'
757 sign. For example, *qrr4*+ expresses only *qrr4,* and the *qrr1, qrr2, qrr3,* and *qrr5* genes are
758 deleted. For each panel, the data shown are from a single experiment that is representative of
759 at least three independent experiments.
760
761 **Figure 6. Virulence phenotypes in DS40M4 and BB120 differ in quorum-**
762 **sensing regulation.** For all panels, assays were performed with *V. campbellii* DS40M4 wild-
763 type, Δ*luxO* (cas197), *luxO* D47E (BDP060), and Δ*luxR* (cas196). (A) Survival of *E.*
764 *coli* in T6SS-dependent killing assays ($n = 9$). (B) Exoprotease activity measured by
765 HPA digestion and normalized to cell density (OD_{600}). ($n = 3$). (C) Biofilm formation measured
766 by crystal violet staining (OD_{595}) normalized to cell density (OD_{600}) ($n = 6$). For all panels,
767 different letters indicate significant differences in 2-way ANOVA of log-transformed data
768 followed by Tukey's multiple comparison's test ($p < 0.05$).
769
770 **Figure 7. Identification of the LuxR regulon and transcriptional start sites in DS40M4**
771 **by differential RNA-Seq.** (A-D) Data shown are qRT-PCR of transcripts of representative
772 quorum sensing-controlled genes in the wild-type, Δ*luxR*, or Δ*qrr1-5* strains. Reactions were
773 normalized to the internal standard (*hfq*). (E) Data shown are cDNA reads from dRNA-seq data

774 mapped to three genetic loci in *V. campbellii* DS40M4 for TEX (-) and TEX (+) samples. Scales
775 are indicated for each panel.
776

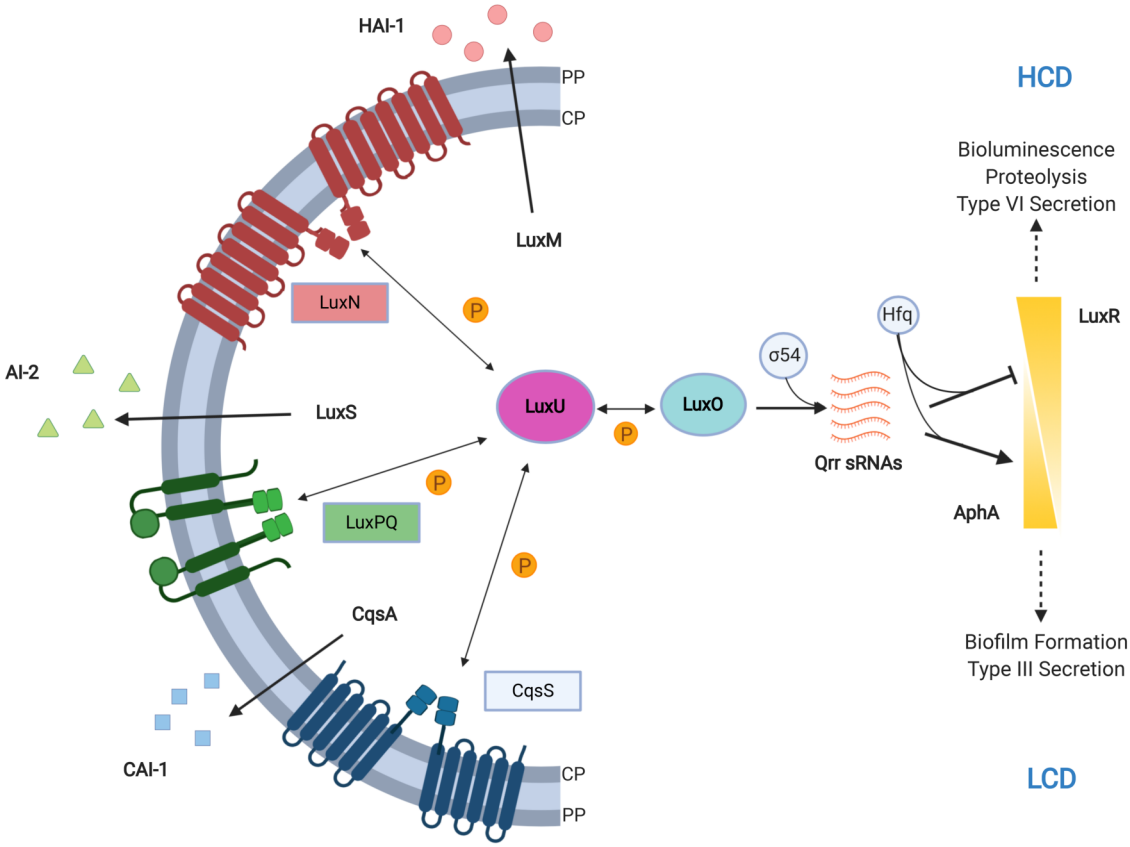

Figure 1: Model for quorum-sensing regulation in *V. campbellii*. The autoinducers CAI-1, HAI-1, AI-2, are produced by autoinducer synthases CqsA, LuxM, and LuxS, respectively. At LCD, autoinducers are at low concentrations, resulting in the receptors acting as kinases. The three receptors phosphorylate LuxU (phosphorelay protein), which transfers the phosphate to LuxO. Phosphorylated LuxO activates *qrr* expression through Sigma-54. The Qrrs together with Hfq bind to the *aphA* and *luxR* mRNAs, and AphA is expressed and LuxR production is minimal. The combination of AphA and LuxR protein levels leads to LCD behaviors, such as type III secretion and biofilm formation. As autoinducers accumulate at HCD, the receptors bind autoinducers and in this state act as phosphatases. De-phosphorylated LuxO does not activate the *qrr* genes, thus leading to maximal LuxR and absence of AphA. This ultimately leads to HCD behaviors such as bioluminescence, proteolysis, and type VI secretion.

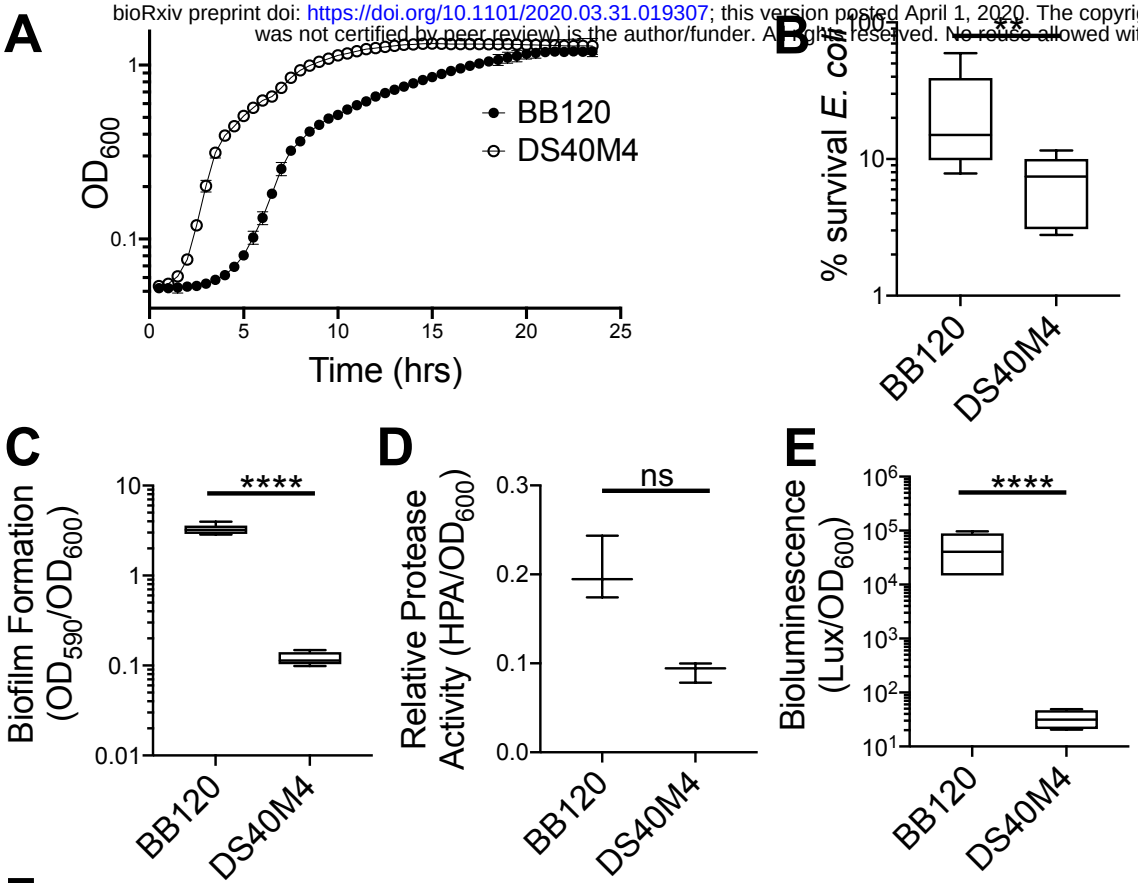

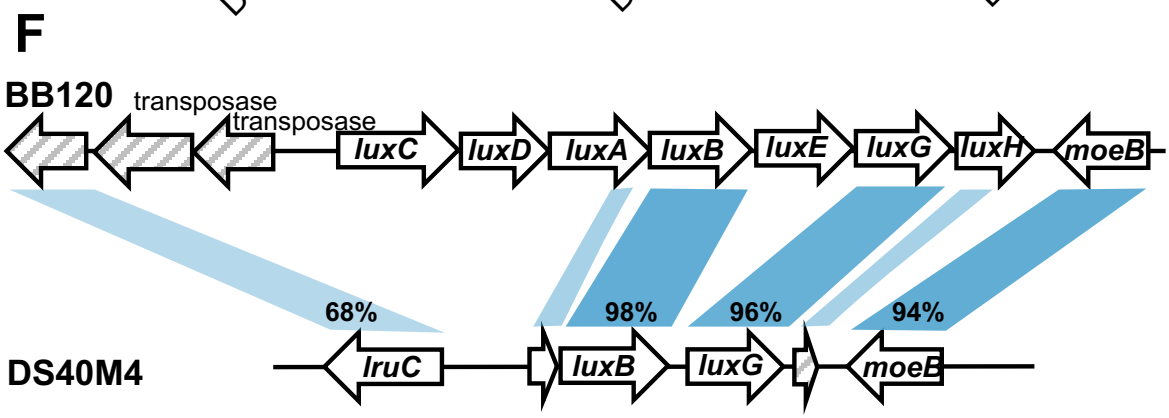

Figure 2: Comparison of growth and virulence-associated phenotypes between BB120 and DS40M4. (A) Growth curve comparing growth rates between BB120 and DS40M4 in LM media. (B) Survival of *E. coli* cells in T6SS-dependent killing assays (n = 9). (C) Biofilm formation measured by crystal violet staining (OD_{595}) normalized to cell density (OD_{600}) (n = 6). (D) Exoprotease activity measured by HPA digestion and normalized to cell density (OD_{600}) (n = 3). (E) Bioluminescence production normalized to cell density (OD_{600}) (n = 4). (F) Diagram indicating the presence of the genes encoding LuxCDABE in BB120 and in DS40M4. For all panels, unpaired, two-tailed t-tests were performed on log-transformed data.

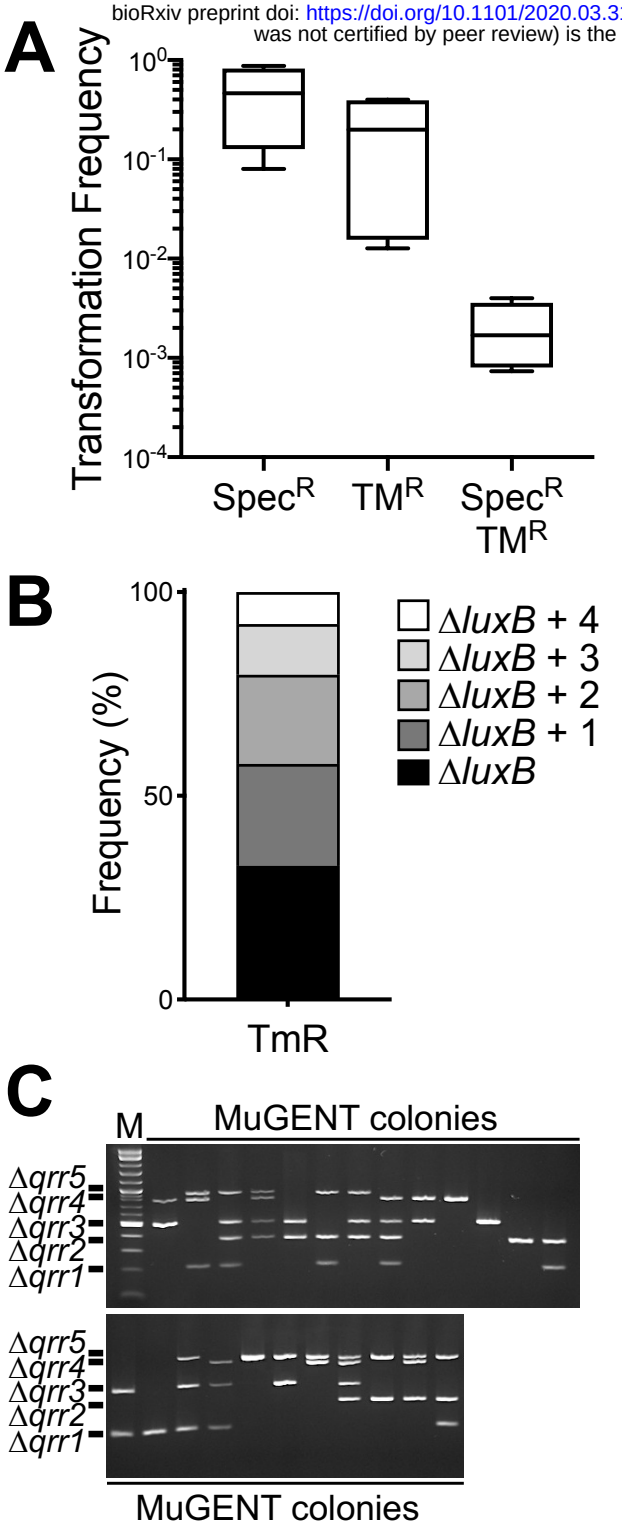

Figure 3. **MuGENT enables deletion of Qrr sRNAs in combinations of up to four unselected mutations.** (A) Co-transformation of linear tDNAs targeting *luxO* (*luxO::spec*^{R}) and *luxR* (*luxR::TM*^{R}). Transformation frequencies are shown for colonies selected on media containing spectinomycin (Spec^{R}), trimethoprim (TM^{R}), or both (Spec^{R}, TM^{R}). (B) Frequency of recovery of the selectable *luxB* deletion alone or in combination with one, two, three, or four *qrr* deletions using MuGENT in DS40M4. (C) Representative agarose gel of 24 MASC-PCR products from transformations targeting all five *qrr* genes *(qrr1-5)* and *luxB* in DS40M4. The presence of a band indicates that the gene has been deleted in that colony.

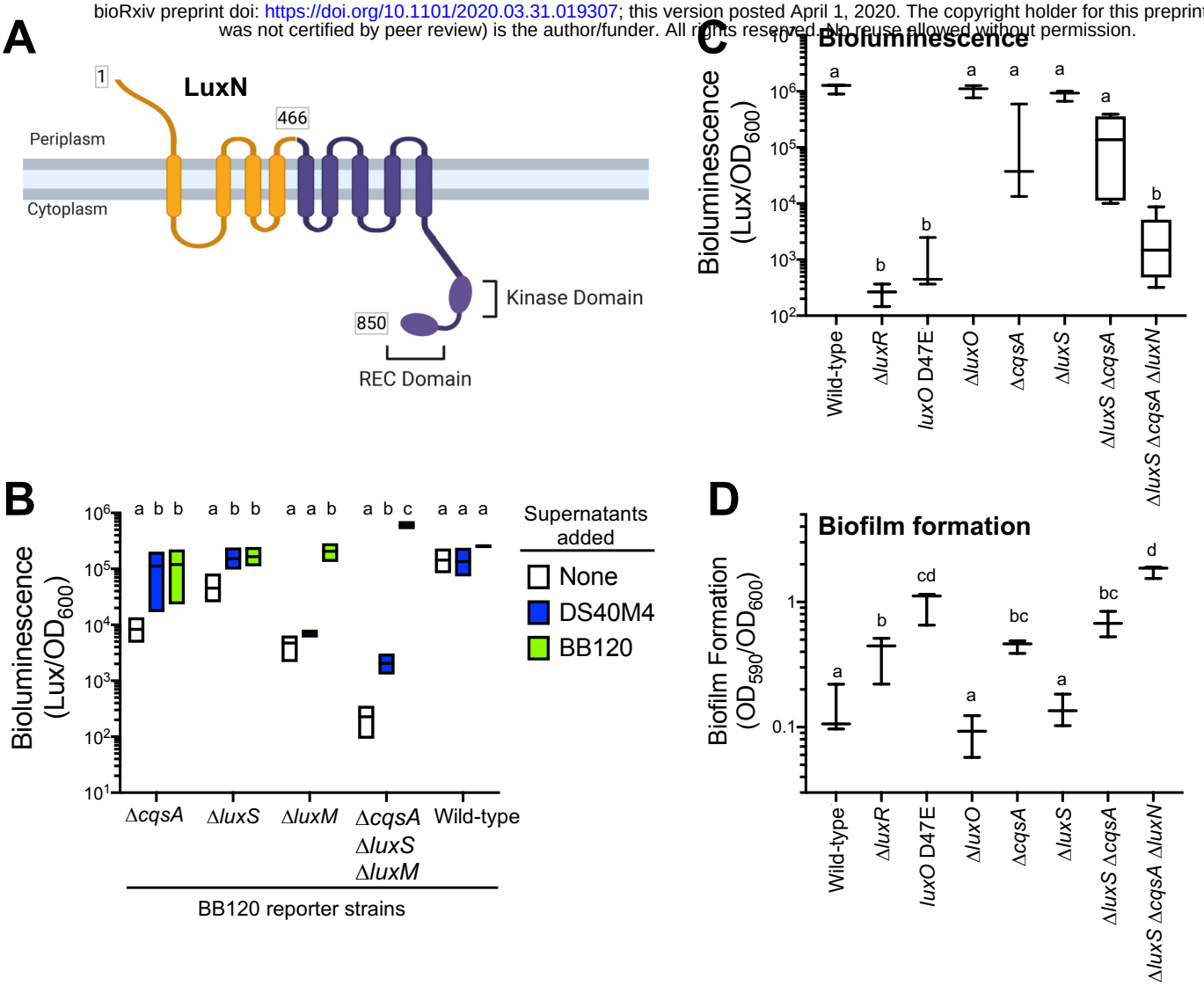

Figure 4. ***V. campbellii*** **DS40M4 produces and responds to CAI-1 and AI-2 autoinducers, but not AI-1.** (A) Diagram of the predicted structure of the DS40M4 LuxN monomer. The conserved C-terminal domain is colored purple, and the N-terminal region that is not conserved is colored orange. (B) Bioluminescence production normalized to cell density (OD_{600}) for strains in which supernatants from the indicated strains were added to BB120 strains. (C) Bioluminescence production normalized to cell density (OD_{600}). (D) Biofilm formation measured by crystal violet staining (OD_{595}) normalized to cell density (OD_{600}). For panels B, C, and D, different letters indicate significant differences in 2-way ANOVA of log-transformed data followed by Tukey's multiple comparison's test ($n = 3$ or $n = 4$, $p < 0.05$). For panel B, statistical comparisons were performed comparing the effects of the three supernatant conditions for each reporter strain; data were not compared between reporter strains.

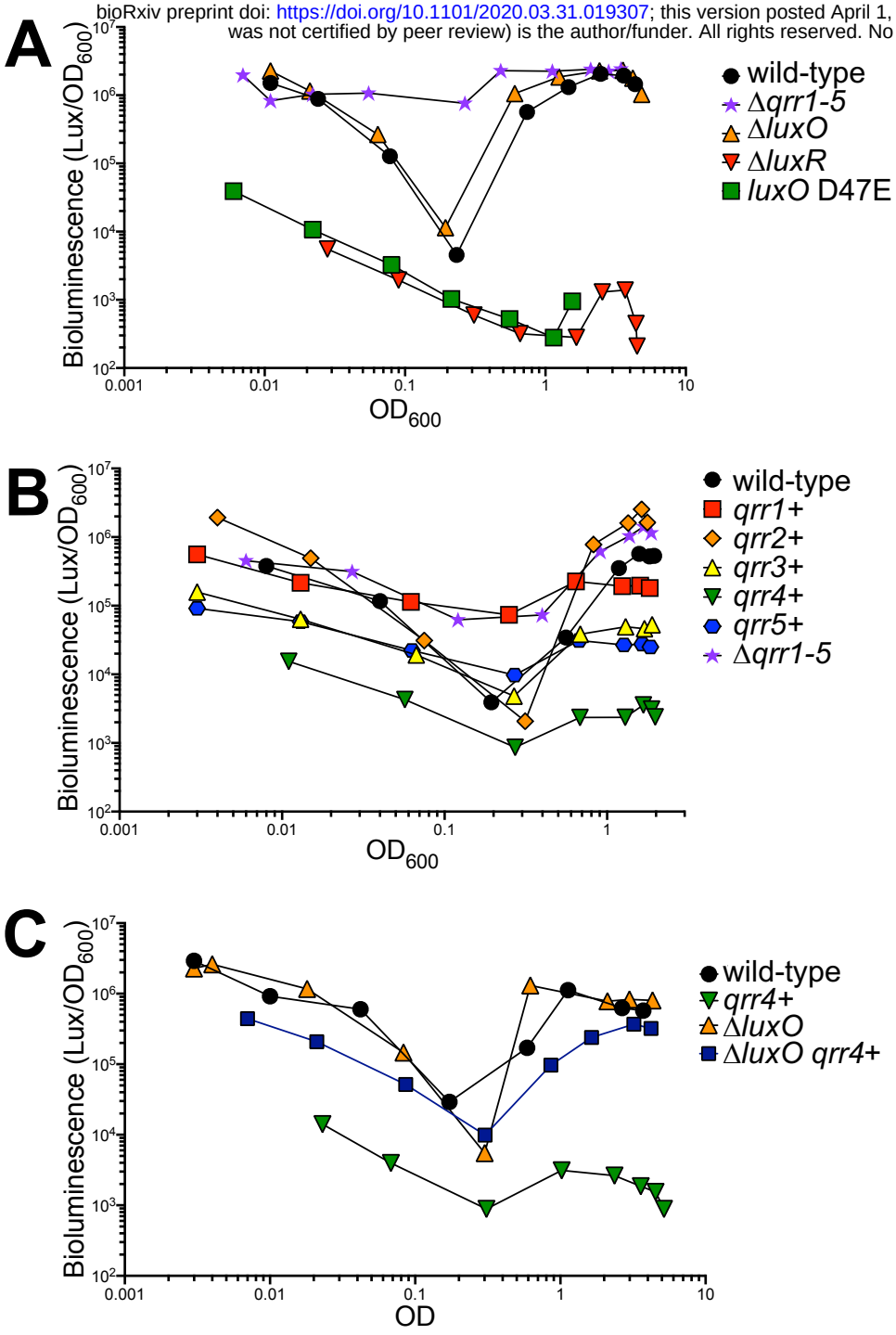

Figure 5. **Quorum sensing regulation of bioluminescence in DS40M4 is distinct from BB120.** For all panels A, B, and C, bioluminescence production is shown normalized to cell density (OD_{600}) during a growth curve. A strain expressing only a single *qrr* is labeled with a '+' sign. For example, *qrr4*+ expresses only *qrr4,* and the *qrr1, qrr2, qrr3,* and *qrr5* genes are deleted. For each panel, the data shown are from a single experiment that is representative of at least three independent experiments.

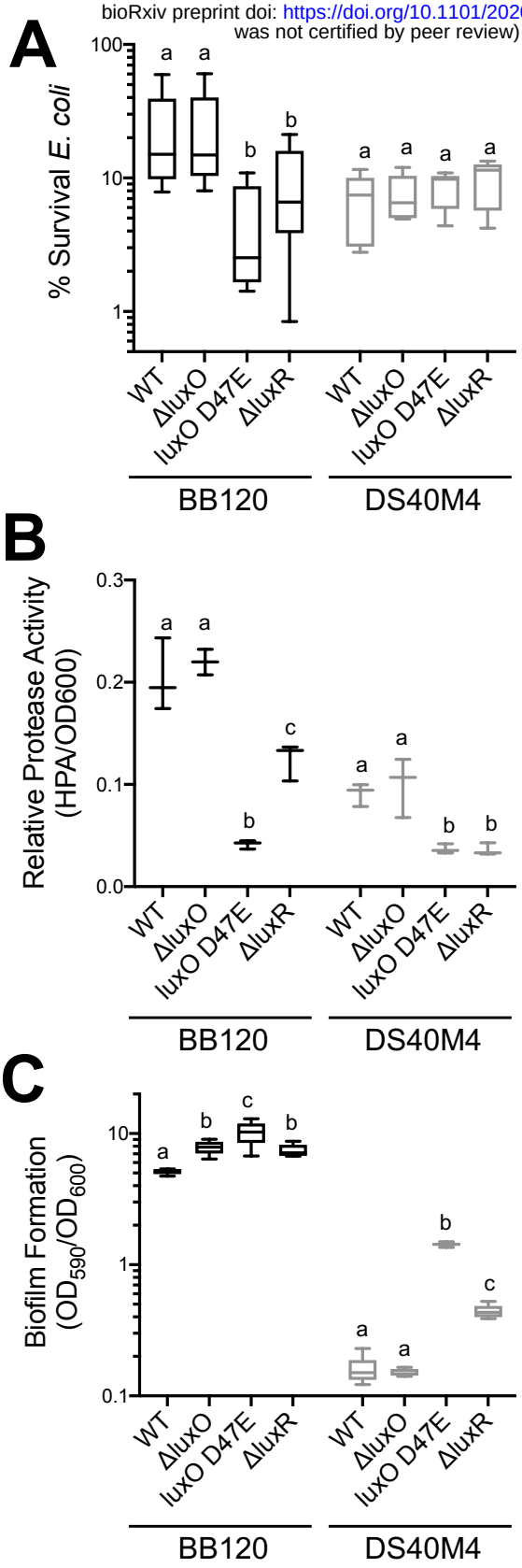

Figure 6. Virulence phenotypes in DS40M4 and BB120 differ in quorum-sensing regulation. For all panels, assays were performed with *V. campbellii* DS40M4 wild-type, Δ*luxO* (cas197), *luxO* D47E (BDP060), and Δ*luxR* (cas196). (A) Survival of *E. coli* in T6SS-dependent killing assays (n = 9). (B) Exoprotease activity measured by HPA digestion and normalized to cell density (OD_{600}). (n = 3). (C) Biofilm formation measured by crystal violet staining (OD_{595}) normalized to cell density (OD_{600}) (n = 6). For all panels, different letters indicate significant differences in 2-way ANOVA of log-transformed data followed by Tukey's multiple comparison's test ($p < 0.05$).

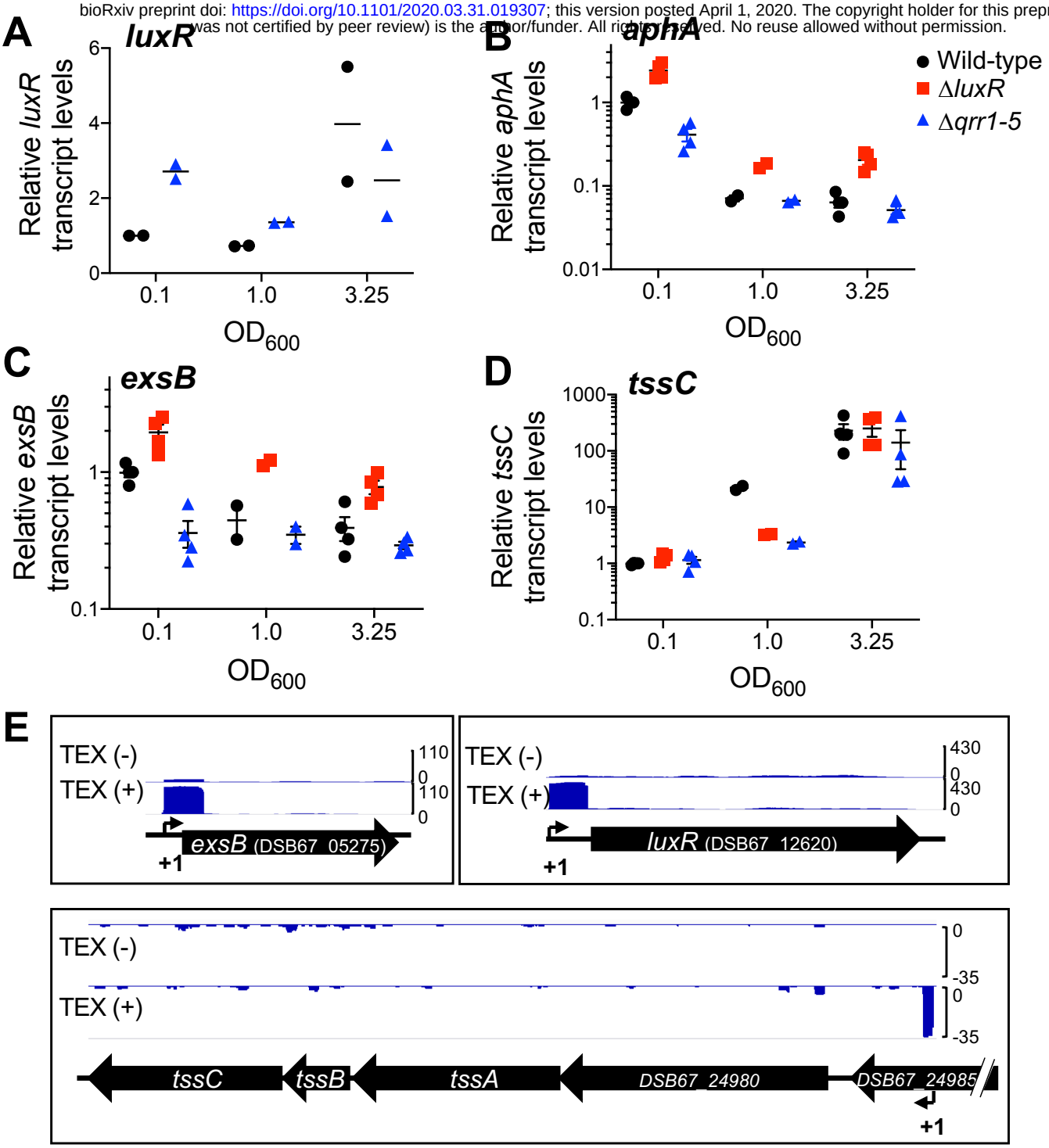

Figure 7. Identification of the LuxR regulon and transcriptional start sites in DS40M4 by differential RNA-Seq. (A-D) Data shown are qRT-PCR of transcripts of representative quorum sensing-controlled genes in the wild-type, Δ*luxR*, or Δ*qrr1-5* strains. Reactions were normalized to the internal standard (*hfq*). *(*E) Data shown are cDNA reads from dRNA-seq data mapped to three genetic loci in *V. campbellii* DS40M4 for TEX (-) and TEX (+) samples. Scales are indicated for each panel.